HHS Public Access

Author manuscript

J Neurochem. Author manuscript; available in PMC 2023 March 01.

Published in final edited form as:

J Neurochem. 2022 March ; 160(6): 613–624. doi:10.1111/jnc.15567.

E3 Ubiquitin Ligase Nedd4-2 Exerts Neuroprotective Effects During Endoplasmic Reticulum Stress

Daphne E Lodes[1], **Jiuhe Zhu**[1], **Nien-Pei Tsai**[1,2,*]

[1]Department of Molecular and Integrative Physiology, School of Molecular and Cellular Biology, University of Illinois at Urbana-Champaign, Urbana, IL 61801, USA

[2]Neuroscience Program, University of Illinois at Urbana-Champaign, Urbana, IL 61801, USA

Abstract

The neural precursor cell expressed developmentally downregulated protein 4-like (Nedd4-2) is an E3 ubiquitin ligase critical for neurodevelopment and homeostasis of neural circuit excitability. While dysregulation of Nedd4-2 has been linked to elevated seizure susceptibility through impaired ubiquitination of multiple direct substrates, it remains largely unclear whether Nedd4-2 interconnects other cellular pathways that affect neuronal activity and seizure susceptibility. Here, we first showed that Nedd4-2 associates with the endoplasmic reticulum (ER) and regulates the expression of multiple ER resident proteins. Further, utilizing *Nedd4-2* conditional knockout mice, we showed that Nedd4-2 is required for the maintenance of spontaneous neural activity and excitatory synapses following the induction of ER stress. When analyzing activation of the canonical pathways of ER stress response, we found that Nedd4-2 is required for phosphorylation of eIF2α. While phosphorylation of eIF2α has been shown to reduce seizure susceptibility, attempts to facilitate phosphorylation of eIF2α in *Nedd4-2* conditional knockout mice failed to produce such a beneficial function, suggesting a role for Nedd4-2 in integrating the ER stress response to modulate seizure susceptibility. Altogether, our study demonstrates neuroprotective functions of Nedd4-2 during ER stress in neurons and could provide insight into neurological diseases in which the expression or activity of Nedd4-2 is impaired.

Graphical Abstract

In *Nedd4-2* conditional knockout (cKO) cortical neuron cultures, induction of endoplasmic reticulum (ER) stress leads to a reduction in spontaneous neural activity, a reduction of excitatory synapses, and impaired eukaryotic initiation factor-2α (eIF2α) phosphorylation. This impairment in eIF2α phosphorylation coupled with *Nedd4-2* deletion in mice causes a defect that impairs pharmacological reduction in seizure susceptibility mediated by salubrinal. These findings uncover neuroprotective functions of Nedd4-2 during ER stress in neurons and could provide insight into neurological diseases associated with impaired *Nedd4-2* activity or an altered ER stress response.

*Correspondence: Nien-Pei Tsai, Ph.D., 407 South Goodwin Ave, Urbana, IL 61801, USA, Tel: 217-244-5620 Fax: 217-333-1133, nptsai@illinois.edu.

AUTHOR CONTRIBUTION

DEL and N-PT designed the research. DEL, JZ, and N-PT performed the experiments and analyzed the data. N-PT acquired the resources for this study. DEL and N-PT wrote the manuscript.

CONFLICT OF INTERST STATEMENT

The authors declare no competing financial interests.

Keywords

Nedd4-2; endoplasmic reticulum; stress; eIF2α; seizure

INTRODUCTION

Nedd4-2, or neural precursor cell expressed developmentally downregulated protein 4-like, is a member of the Nedd4 family of HECT type E3 ubiquitin ligases (Donovan and Poronnik 2013). Members of this family maintain a highly conserved structure, with a lipid-binding C2 domain at the N-terminus, several WW domains which mediate substrate binding and affinity, and a catalytic HECT domain at the C-terminus (Ingham *et al.* 2004). As an E3 ubiquitin ligase, the primary function of Nedd4-2 is to target substrates for ubiquitination in order to mediate protein expression or localization. Nedd4-2 is highly expressed in several tissues, including the liver, kidney, heart, lung, and brain (Yanpallewar *et al.* 2016; Goel *et al.* 2015).

Previously, Nedd4-2 has been implicated in a variety of diseases including cardiac abnormalities, cystic fibrosis, hypertension, kidney disease, epilepsy, and stroke (Manning and Kumar 2018; Lackovic *et al.* 2012). In many of these instances, the relationship between Nedd4-2 and disease pathophysiology is well explained by the improper ubiquitination of specific targets of Nedd4-2. For instance, Liddle syndrome is a hereditary form of early onset hypertension that is caused by mutations in the epithelial sodium channel (ENaC) (Rotin 2008). These mutations are in the PY motif of ENaC, which impairs substrate recognition and ubiquitination by Nedd4-2 (Shi *et al.* 2008). In the instance of stroke, researchers have found that amongst members of the Nedd4 family, Nedd4-2 is selectively upregulated in response to ischemic injury (Lackovic *et al.* 2012). Further, when Nedd4-2 upregulation is impaired by genetic knock-down, ischemic injury is more severe and appears to be mediated by ubiquitination of synuclein (Kim *et al.* 2020). Lastly, several epilepsy associated mutations of Nedd4-2 have been identified in human patients (Dibbens *et al.* 2007). These mutations have been shown to impair the ability of Nedd4-2 to ubiquitinate the GluA1 subunit of the AMPA receptor, thereby increasing neuronal excitability (Zhu *et al.* 2017).

In each of the above examples, the function of Nedd4-2 in mediating disease pathophysiology is neatly tied to the dysregulation of a specific protein. Interestingly, however, there is an emergence of research suggesting that Nedd4-2 is differentially activated and regulated in response to a variety of cellular stressors. For instance, Nedd4-2 has been shown to regulate OGG1 protein levels in response to DNA damage, which may have implications for DNA repair capacity (Hughes and Parsons 2020). In a study investigating mechanisms of heart failure, it was found that oxidative stress down-regulates the expression of Nedd4-2 to impair TrkA ubiquitination, which in turn promotes cAMP signaling that modulates heart activity (Wang *et al.* 2021). In another study looking at the cellular response to oxidative stress, it was found that decreased Nedd4-2 expression at the mRNA transcript level promotes stability of a protein called LATS1 which facilitates cell death in response to oxidative stress (Rajesh *et al.* 2016). As it relates to autophagy, Nedd4-2

expression has been differentially shown to promote or inhibit autophagy depending on the cell type (Wang *et al*. 2016; Lee *et al*. 2020). Importantly, the breadth of these studies suggests that the response of Nedd4-2 to stressors occurs in a cell specific manner, as well as a pathway specific manner. Only one study investigating the role of Nedd4-2 in the endoplasmic reticulum (ER) stress response has been conducted in neurons. In this study, it was found that Nedd4-2 is differentially phosphorylated in response to ER stress and contributes to translational suppression (Eagleman *et al*. 2020). Because the cellular stress response is commonly dysregulated in neurological diseases, it is important to gain a further understanding of the activity and regulation of Nedd4-2 in neurons under cellular stress.

In this study, we conducted biochemical and physiological experiments to determine whether Nedd4-2 may play a neuroprotective role during ER stress. We provide evidence that Nedd4-2 interacts with the ER and regulates the expression of ER resident proteins. Physiologically, we show that brain-specific conditional knockout of *Nedd4-2* in mice (Nedd4-2 cKO mice) leads to changes in neural activity and the number of excitatory synapses during ER stress. Molecularly, we reveal that *Nedd4-2* cKO mice exhibit impairments in the phosphorylation of eIF2α, an important pathway in the unfolded protein response (UPR). Furthermore, while pharmacologically promoting phosphorylation of eIF2α can reduce seizure susceptibility in WT mice as shown previously (Kim *et al*. 2014; Sokka *et al*. 2007), *Nedd4-2* cKO mice fail to show such a response. Altogether, our study demonstrates a critical and protective role for Nedd4-2 during ER stress in neurons and could provide insight into diseases in which the expression or activity of Nedd4-2 is dysregulated.

MATERIALS AND METHODS

This study was not preregistered. To minimize animal suffering and the number of animals used, all experiments using animal data followed the guidelines of *Animal Care and Use* provided by the University of Illinois Institutional Animal Care and Use Committee (IACUC) and the guidelines of *Euthanasia of Animals* provided by the American Veterinary Medical Association (AVMA). This study was performed under an approved IACUC animal protocol at the University of Illinois at Urbana-Champaign (#20049 to N.-P. Tsai).

Animals

Wild type (WT) (RRID: IMSR JAX: 000664) and *Emx1-Cre* (RRID: IMSR JAX: 022762) mice in C57BL/6J background were obtained from The Jackson Laboratory. *Nedd4-2* floxed mice were obtained from Dr. Hiroshi Kawabe (Max Planck Institute, Göttingen, Germany). The animals were housed in standard cages on a 12 hr light-dark cycle with ad libitum access to food and water. For primary cortical neuron cultures, newborn mice at postnatal (P) day 0–1 were anesthetized by hypothermia, induced by placing the pups over a piece of aluminum foil on ice for two minutes. Following anesthesia, the mice were decapitated by scissors. For seizure experiments, we utilized mice at six to eight weeks of age. Genotyping was performed for both the *Nedd4-2* loxP and *Emx1-Cre* alleles using PCR as described previously (Zhu *et al*. 2019). The timeline of experimental procedures is summarized in Figure 1A.

Reagents

Bovine serum albumin (BSA) was from Fisher Scientific (catalog: BP9706-100). Dimethyl sulfoxide (DMSO) was from Fisher Scientific (catalog: BP231-100). Thapsigargin was from Adipogen (catalog: AG-CN2-0003). Salubrinal was from Sigma Aldrich (catalog: SML0951). Saline was from Hanna Pharmaceutical (catalog: NC9054335). Kainic acid was from Cayman Chemical Company (catalog: 78050). The antibodies used in this study were purchased from ProteinTech (anti-Gapdh, RRID: AB_2107436), AbClonal (anti-XBP1 [RRID: AB_2757016] and anti-ATF6 [RRID: AB_2801582]), Abcam (anti-Synapsin I [RRID: AB_2200097], anti-PSD-95 [RRID: AB_303248], and anti-Map2 [RRID: AB_2138147]) and Cell Signaling (anti-Nedd4-2 [RRID: AB_1904063], anti-eIF2α [RRID: AB_10692650], anti-phospho-eIF2α [RRID: AB_2096481], anti-PDI [RRID: AB_2156433], anti-COX IV [RRID: AB_2797784], anti-IRE1α [RRID: AB_823545], and anti-ATF4 [RRID: AB_2616025]).

Proteomics

The proteomic screening was conducted using total membrane fractions of *Nedd4-2* WT (Nedd4-$2^{f/f}$ Cre^{-}) and *Nedd4-2* conditional knockout (cKO; Nedd4-$2^{f/f}$ Cre^{+}) mouse brains with label-free analysis provided by Bioproximity. The membrane protein extraction was conducted using the Mem-PER Plus Membrane Protein Extraction Kit (Thermo Scientific; catalog: 89842) (Zhu *et al*. 2019). Following membrane protein extraction, trypsin was added at a ratio of 1:50 to the samples, which were then incubated at 37°C overnight. Then, the peptides were extracted, lyophilized, and resuspended in 2–20 μL of 0.1% formic acid. Ultra-performance liquid chromatography-tandem mass spectrometry (UPLC-MS/MS) was done using the Easy-nLC1200 and HF-X Hybrid Quadropole-Orbitrap mass spectrometer. The relative protein abundance was determined by the chromatographic peak intensity measurements, done by aligning the chromatographic peaks of precursor ions. The relative intensity of each of the identified proteins from the sample sets were normalized to the intensity of β-actin. The mean and the subsequent standard deviation from the mean, used to create the heat maps, were derived from the pooled average of individual genes from all samples. The raw data files were analyzed and searched against the Uniprot-*Mus musculus* protein databases.

Primary Neuron Cultures

Primary cortical neuron cultures were made from mixed-sex mice at postnatal (P) day 0–1. Briefly, cortices were dissected, isolated, and triturated. Cells obtained through this preparation were plated with Dulbecco's Modified Eagle Medium (DMEM). Four to six hours later, the DMEM was removed and neurons were subsequently maintained in NeuralA basal medium (Thermo Fisher, catalog: 10888022) supplemented with B27 supplement (Invitrogen, catalog: 17504001), GlutaMax (2 mM; Invitrogen, catalog: 35050061), penicillin/streptomycin (100 IU/mL of penicillin and 100 μg/mL of streptomycin; Thermofisher, catalog: 30002CI), and cytosine ß-D-arabinofuranoside (AraC, 2 μM; Sigma, catalog: C1768-100MG). Half of the culture medium was replaced with fresh medium every three to four days thereafter until the experiments were conducted on days-in-vitro (DIV)

12–14. Each experiment in this study was performed with at least three independent litters and cultures.

Western Blotting

Protein samples for western blotting were mixed in a sodium dodecyl sulfate (SDS) buffer (40% glycerol; 240 mM Tris-HCl, pH 6.8; 8% sodium dodecyl sulfate; 0.04% bromophenol blue; and 5% β-mercaptoethanol) and boiled for five minutes. After cooling on ice, the samples were loaded onto either 8%, 10%, or 12% sodium dodecyl sulfate polyacrylamide gel electrophoresis gels. After gel electrophoresis, the gel was transferred onto a polyvinylidene fluoride membrane. The membrane was blocked with 1% bovine serum album solution in Tris-buffered saline Tween-20 buffer (TBST; [20 mM Tris, pH 7.5; 150 mM NaCl; 0.1% Tween-20]) and then incubated overnight with primary antibody at 4°C. Following the overnight incubation, the membrane was washed three times for ten minutes in TBST and then incubated with an HRP-conjugate secondary antibody (anti-mouse IgG from Cell Signaling, RRID: AB_330924; anti-rabbit IgG from Jackson Immuno Research, RRID: AB_10015282) in 5% nonfat milk in TBST for one hour at 22°C. Three additional ten minute washes with TBST were performed. The membranes were developed using an enhanced chemiluminescence reagent.

Isolation of rough endoplasmic reticulum from mouse whole brain lysates.

This whole procedure was performed on ice or at 4°C. Solutions were cooled prior to use. Briefly, fresh brains from WT mice were collected and washed twice for three minutes in 10 mL of PBS. After washing, the tissue was transferred to a glass homogenizer and manually homogenized in 3.5 mL of an isotonic extraction buffer (10 mM HEPES, pH 7.8; 250 mM sucrose; 25 mM potassium chloride; and 1 mM EGTA) and protease inhibitor. The homogenized sample was transferred to a 15 mL centrifuge tube and centrifuged at 1,000g for 10 minutes at 4°C. Following centrifugation, the thin floating lipid layer was removed by aspiration, with care taken not to aspirate the post-nuclear supernatant. The post-nuclear fraction was transferred to another centrifuge tube and centrifuged at 12,000g for 15 minutes at 4°C. Again, the floating lipid layer was removed by aspiration with care taken not to aspirate the post-mitochondrial supernatant. The post-mitochondrial fraction, the source of microsomes, was then transferred to a new Eppendorf tube and the volume measured. A volume of 8 mM calcium chloride 7.5 times the volume of the post-mitochondrial fraction was added to the post-mitochondrial fraction dropwise with constant stirring. Following addition of the calcium chloride solution, the sample was stirred for an additional 15 minutes at 4°C. After stirring, the sample was centrifuged at 8,000g for 10 minutes at 4°C, with rough ER enriched microsomes found in the pellet following centrifugation. The supernatant was removed and microsomes were resuspended in the isotonic extraction buffer. Throughout the isolation process, samples were taken of the total brain lysate, post-nuclear fraction, post-mitochondrial fraction, and rough ER enriched microsome isolation. The samples were used for western blotting to confirm the presence of Nedd4-2, as well asto verify the efficiency of the isolation protocol.

Immunocytochemistry and Confocal Microscopy

Primary cortical neurons were made from mixed-sex WT, *Nedd4-2* WT, and *Nedd4-2* cKO mice at P0 or P1 as described previously on glass coverslips at a density of 1.5×10^5 cells (to investigate ER colocalization) and 1.25×10^5 cells (to count synapses) per coverslip, counted using a hemocytometer (Lee *et al.* 2018). At DIV14, cells were washed once with phosphate buffered saline (PBS), fixed with fixation buffer (4% paraformaldehyde and 4% sucrose in PBS) for 15 minutes, and then permeabilized with 0.5% Triton-X-100 in PBS for five minutes at room temperature. Following fixation and permeabilization, the neurons were incubated overnight with antibodies in 1% BSA in PBS. For those experiments looking at Nedd4-2 colocalization with the ER, the coverslips were incubated with antibodies against Nedd4-2, PDI, and Map2. For those experiments counting synapses, neurons were incubated with antibodies against synapsin I, PSD-95, and Map2. Following the overnight incubation, the samples were washed three times for ten minutes each with PBS, incubated with fluorescence conjugated secondary antibodies (goat anti-rabbit IgG cross-Adsorbed Secondary Antibody Alexa Fluor 488 [Thermo Fisher Scientific, RRID: AB_143165], goat anti-mouse IgG Cross-Adsorbed Secondary Antibody Alexa Fluor 555 [Thermo Fisher Scientific, RRID: AB_2535844], and goat anti-chicken IgG Cross-Adsorbed Secondary Antibody Alexa Fluor 633 [Thermo Fisher Scientific, RRID: AB_2535756]) for two hours at room temperature in 1% BSA in PBS, and then were washed an additional three times for ten minutes each with PBS. The coverslips were then mounted onto glass slides.

Images were obtained using a Zeiss LSM 700 confocal microscope with 40x magnification and three different laser lines (488, 555, and 633 nm). The pinhole was set to 1 airy unit for all experiments. The confocal microscope settings were maintained with the same laser and scanning configurations to allow for comparison across conditions. For image analysis, ImageJ software was used to quantify the number of synapses in secondary dendrites based on intensity correlation of synapsin I and PSD-95 signals. Measurements were only taken from neurons in which two to three secondary dendrites were present.

MEA Recordings

Recordings were done at DIV12–14 in the same culture medium using an Axion Muse 64-channel system in single well MEA dishes (M640GL1–30pt200, Axion Biosystems) inside a 5% CO_2, 37°C incubator. Each plate was coated with poly-D-lysine for at least one hour prior to plating. The neurons were plated at a density of $1{\times}10^5$, counted using a hemocytometer. Field potentials (voltage) at each electrode were recorded at a sampling rate of 25 kHz. After 30 minutes of baseline recording, each MEA dish was treated with the drugs specified and then recorded for another 30 minutes at the end of the treatment time. Due to changes in network activity caused by physical movement of the MEA, only the last 15 minutes of each recording were used for data analysis. To ensure consistency when acquiring MEA data, all experimental procedures ranging from animal dissection, cell counting and plating, medium changing, and recording were conducted by the same individual for each experiment. For all drug treatment comparisons, the recording for each MEA culture after treatment was directly compared to the baseline recording of the same culture in order to minimize variability between cultures.

All data was analyzed using AxIS Software (Axion Biosystems). To extract spikes (i.e. action potentials) from the raw electrical signal, a threshold of ± 7 standard deviations was independently set for each channel; any activity beyond this threshold was counted as a spike. Only MEAs with more than 2,000 spikes measured during the last 15 minutes of the pre-recording were included for data analysis. The total number of spikes obtained from each culture was normalized to the number of electrodes. To extract information about bursting behavior from the raw electrical signal, bursts were recognized in each electrode as a minimum of five spikes with a maximum inter-spike interval of 0.1 seconds. From this data, the AxIS software analyzed the burst duration, number of spikes per burst, and interburst interval (i.e. burst frequency). The synchrony index of each MEA dish was computed through the AxIS software, based on a published algorithm used previously within our lab, by taking cross-correlation between any two spike trains, removing the portions of the cross-correlogram which are contributed to auto-correlations of the spike train, and reducing the distribution to a single metric. A value of 0 corresponds to no synchrony within the culture, and a value of 1 corresponds to perfect synchrony within the culture.

Intraperitoneal injections, seizure induction, and seizure activity test

Male mice between 6 to 8 weeks of age were intraperitoneally injected twice (once 20 hours prior to seizure induction and once 30 minutes prior to seizure induction) with salubrinal prepared in saline solution (Hannas Pharmaceutical) with 1% DMSO, at a dose of 1 mg/kg (Hossain *et al.* 2019). Mice would be excluded from data analysis if they died after receiving the salubrinal injections. Thirty minutes after the second salubrinal injection, the mice were intraperitoneally injected with kainic acid, prepared in saline solution, at a dose of 15 mg/kg (Zhu *et al.* 2017). The total injection volume was kept close to 0.1 mL as described previously (Liu *et al.* 2019). After injection with kainic acid, the mice were closely observed in real time for four hours. The intensity of seizures was assessed by a modified Racine's scoring system (Lüttjohann *et al.* 2009).

Experimental Design and Statistical Analysis

For dissociated neuronal cultures, cortices derived from 3–4 pups from a single litter were pooled before plating. At least 3 litters were used in each experiment; the figure legends provide specific information regarding the number of litters or mice used for each experiment. The expected sample size was estimated based on our previous studies (Zhu *et al.* 2019; Eagleman *et al.* 2020). No randomization was performed to allocate subjects in this study. Because of the design of our research, no blinding was performed. For experiments utilizing cortical neuron cultures, each experiment was performed and analyzed using sister cultures made from the same litter. For experiments utilizing mice, littermate controls were used as appropriate. The data presented in this study have been tested for normality using Kolmogorov-Smirnov Test. We used ANOVA with *post-hoc* Tukey HSD (Honest Significant Differences) tests were used for multiple comparisons between treatments or genotypes. The two-tailed Student's *t*-test was used for western blotting results when two conditions were compared. Outliers were determined using GraphPad Outlier calculator, which performs the Grubbs' test. Specific sample numbers are indicated in the figure legends. Differences are considered significant at the level of $p < 0.05$.

RESULTS

Nedd4-2 associates with the ER.

We first aimed to determine if there is evidence to suggest that Nedd4-2 may play a regulatory role within the ER in neurons. To this end, we first confirmed an association between Nedd4-2 and the ER. Rough ER enriched microsomes were collected via differential centrifugation and calcium chloride precipitation from WT mouse brains. We conducted western blotting against the various fractions obtained during the preparation, including the total brain fraction, post-nuclear fraction, post-mitochondrial fraction, and rough ER enriched microsomal fraction (Figure 1B) with Nedd4-2, PDI (a positive marker for endoplasmic reticulum), and CoxIV (a positive marker for mitochondria). Here, we were able to show that our preparation produced a rough ER microsomal fraction free of contamination by other organelles and that Nedd4-2 is indeed present in the rough ER enriched microsomal fraction. To further confirm an association between Nedd4-2 and the ER *in situ*, we conducted immunocytochemistry utilizing WT primary cortical neuron cultures. We used PDI as an ER marker and observed colocalization between PDI and Nedd4-2 (Figure 1C). Taken together, these two methods support the notion that Nedd4-2 associates with the ER.

We then asked whether Nedd4-2 may play a role in ER function. To this end, we utilized an unbiased proteomic approach to identify dysregulation of ER associated proteins in the absence of Nedd4-2 (Eagleman *et al.* 2020). We obtained total membrane fractions, using Mem-PER Plus Membrane Protein extraction reagents from whole brains derived from *Nedd4-2* WT (Nedd4-$2^{f/f}$ Cre^{-}) and *Nedd4-2* cKO (Nedd4-$2^{f/f}$ Cre^{+}) mice for quantitative proteomic profiling. We focused on membrane fractions for two reasons; first, because the ER is a network of membranes, it was beneficial to collect membrane fractions to enrich the population of ER associated proteins, and second, it is understood that Nedd4-2 has an affinity towards interacting with and ubiquitinating membrane-bound proteins (Zhu *et al.* 2019). Using littermate controls for each genotype, we obtained quantitative measurements for a total of 1,228 proteins. Utilizing COMPARMENTS (https://compartments.jensenlab.org/Search), we identified 166 of these 1,228 proteins as being localized within the ER at a confidence score of 3 or above (Binder *et al.* 2014). Of these proteins, 44 endoplasmic reticulum associated proteins were identified as exhibiting a 50% increase (1.5 fold) or a 33% reduction (0.67 fold) in *Nedd4-2* cKO samples compared to *Nedd4-2* WT samples (Figure 1D). This result suggests that Nedd4-2 may have a physiological function associated with the ER.

Spontaneous neural activity decreases in Nedd4-2 cKO neurons upon induction of ER stress.

To begin to understand whether Nedd4-2 plays a role when ER homeostasis is disturbed, we challenged primary cortical neuron cultures derived from *Nedd4-2* WT and *Nedd4-2* cKO mice with a chemical inducer of ER stress, thapsigargin (Tg). Tg induces ER stress by inhibiting the sarco/endoplasmic reticulum calcium ATPase (SERCA), which typically functions to sequester calcium ions within the endoplasmic reticulum. We began by investigating whether ER stress induced any alterations in neural network activity. To

address this question, we utilized a multielectrode array (MEA) system to measure the spontaneous activity of cultures derived from *Nedd4-2* WT and *Nedd4-2* cKO brains. Beginning at DIV 12–14, the spontaneous activity of the cortical neuron cultures was recorded prior to the treatment. Then, the cultures were challenged with Tg (1 μM) or a vehicle control (DMSO) for four hours. Following the treatment period, the spontaneous activity was recorded and directly compared to its baseline activity.

We investigated whether there were any changes in neural activity after ER stress, including changes in spontaneous spike rate, spike amplitude, bursting activity as measured by burst duration, number of spikes per burst, and burst frequency, and changes in the cross-electrode synchronization. We observed genotype specific differences in the spontaneous spike rates after induction of ER stress (Figure 2A–B). In *Nedd4-2* WT cultures, there was no significant change in the spontaneous spike rate after treatment with Tg; however, in *Nedd4-2* cKO cultures, there was a significant reduction in the spontaneous spike rate (Figure 2B). We did not observe any significant differences in spontaneous spike amplitude (Figurer 2C), the metrics of bursting activity (Figure 2D–F) or synchronization (Figure 2G). Although previous research from our lab has demonstrated basally elevated spontaneous spike rates in cultured neurons that are genetically deficient in Nedd4-2 (Zhu *et al.* 2017), an effect which is correlated with elevated seizure susceptibility, our current findings indicate that *Nedd4-2* cKO neurons are less capable of maintaining spontaneous spike rate during ER stress.

Nedd4-2 is required to maintain the number of excitatory synapses upon induction of ER stress.

Spontaneous activity in a neural network can be affected by neuronal intrinsic excitability and synaptic connectivity. Because we did not observe changes in bursting activity (Figure 2D–F) and our previous work suggests no detectable effects on intrinsic neural excitability following acute induction of ER stress (Liu *et al.* 2021a), we asked whether Nedd4-2 functions to maintain synaptic connections during ER stress. On DIV 12–14, we treated *Nedd4-2* WT and *Nedd4-2* cKO cortical neuron cultures with Tg or DMSO for four hours. Following treatment, the neurons were permeabilized, fixed, and stained with synapsin I and PSD-95, pre- and post- synaptic markers respectively, to measure colocalization of pre- and post- synaptic puncta. As shown in Figure 3, *Nedd4-2* WT cultures challenged with Tg showed no significant changes in synaptic puncta number; however, *Nedd4-2* cKO cultures showed a significant decrease in synaptic puncta number. These results suggest that Nedd4-2 is required to maintain the number of excitatory synapses upon induction of ER stress.

Phosphorylation of eIF2α is impaired in the absence of Nedd4-2 upon induction of ER stress.

In response to ER stress, cells activate a canonical signaling pathway known as the unfolded protein response (Hetz 2012). Because we observed impaired physiological responses following induction of ER stress in *Nedd4-2* cKO neurons (Figures 2–3), we asked whether Nedd4-2 is also required for activation of the UPR. To answer this question, we utilized primary cortical neuron cultures derived from *Nedd4-2* WT and *Nedd4-2* cKO mice. At DIV 12–14, the cultures were treated with Tg (1 μM) for four hours and western blotting was

conducted against various UPR markers, including IRE1α, XBP1 (spliced and unspliced), ATF6 (cleaved and uncleaved), phosphorylated-eIF2α and eIF2α, and ATF4.

We first looked at activation of the PERK signaling pathway as measured by phosphorylation of eIF2α (Figure 4A). In response to treatment with Tg in *Nedd4-2* WT cultures, we observed a significant increase in eIF2α phosphorylation, confirming that our treatment paradigm is sufficient to induce the ER stress response. Interestingly, however, the same treatment in *Nedd4-2* cKO cultures did not elicit a significant increase in eIF2α phosphorylation. When evaluating ATF4, a protein that is positively regulated by phosphorylated eIF2α, we also observed a stronger induction of ATF4 in *Nedd4-2* WT cultures in comparison to that observed in *Nedd4-2* cKO cultures (Supplemental Figure S1). These results suggest that Nedd4-2 is required for phosphorylation of eIF2α upon induction of ER stress.

When we focused on activation of the IRE1α signaling pathway, we were surprised to find that this arm of the unfolded protein response does not appear to be activated in the timeline of our treatment paradigm, as determined by no changes in IRE1α expression and no observable splicing or changes in total expression of XBP1 (Figure 4B). Because we did not observe the spliced form of XBP1, we chose to quantify total expression of XBP1. When we focused on activation of the ATF6 signaling pathway, we had similar results. We did not observe any ATF6 cleavage product in our western blotting, and as a result quantified changes in total expression of ATF6 (Figure 4C). There were no changes based on treatment or genotype. In summary, our data reveal an elevation of eIF2α phosphorylation in cultured cortical neurons under ER stress, and suggest that Nedd4-2 is required for this effect.

eIF2α phosphorylation-dependent reduction of seizure susceptibility in impaired in Nedd4-2 cKO mice.

Several studies have shown that genetic deficiency of Nedd4-2 expression increases seizure susceptibility in mice (Zhu *et al.* 2017; Liu *et al.* 2021b). Although these studies investigated possible targets of Nedd4-2 that may mediate this increase in basal seizure susceptibility, it remains possible that additional pathways are involved. A previous study has shown that eIF2α phosphorylation is increased in the brain following seizure insult (Carnevalli *et al.* 2006). Further, other studies have shown that pre-treatment with salubrinal, an inhibitor of eIF2α phosphatases, prior to seizure induction with kainic acid can reduce seizure severity (Kim *et al.* 2014; Sokka *et al.* 2007). Because we observed deficits in eIF2α phosphorylation in *Nedd4-2* cKO cultures, we asked whether mediating this pathway might have any impact on seizure severity or seizure susceptibility in *Nedd4-2* cKO mice.

We answered this question by administering two intraperitoneal (i.p.) injections of salubrinal (1 mg/kg) 20 hours and 30 minutes before seizure induction to *Nedd4-2* WT and *Nedd4-2* cKO mice. Seizures were induced with a single injection of kainic acid (15 mg/kg) (Zhu *et al.* 2017) and the mice were observed for a total of four hours. The low dose of kainic acid was chosen to avoid mortality based on our previous work (Liu *et al.* 2019). We scored the mouse seizure behavior every 15 minutes according to a modified Racine's scale (Liu *et al.* 2019). We then quantified the intensity of seizures experienced by these mice by calculating the area under the curve according to the trapezoidal rule (Kang *et al.* 2018; Johnston *et*

al. 2014). Here, we found that *Nedd4-2* WT mice pre-treated with salubrinal showed a significant reduction in seizure severity (Figure 5A) and a reduced time of overall seizure burden (Figure 5B). This finding aligns well with previous studies suggesting a beneficial role for salubrinal pre-treatment prior to seizure induction (Kim *et al*. 2014; Sokka *et al*. 2007). However, when we quantified the seizure activity of *Nedd4-2* cKO mice, we did not find any significant changes in seizure intensity or time of seizure burden. Because Nedd4-2 cKO neurons do respond to salubrinal, as confirmed by elevation of eIF2α phosphorylation after treatment (Supplemental Figure S2), we suggest that the absence of Nedd4-2 uncouples eIF2α phosphorylation from the regulation of seizure susceptibility.

DISCUSSION

This current study aimed to determine whether Nedd4-2 plays a role in ER function by investigating the physiological consequences of Nedd4-2 deletion in response to ER stress. As shown in Figure 6, through our work we confirmed that Nedd4-2 interacts with the ER and provided evidence to suggest that Nedd4-2 regulates the expression of ER resident proteins. Further, we showed that Nedd4-2 deficiency leads to a reduction in neural activity and the number of excitatory synapses in response to ER stress. We also showed that Nedd4-2 deficiency impairs ER stress-induced phosphorylation of eIF2α and eIF2α phosphorylation-dependent reduction of seizure susceptibility. These results from our study establish a critical role for Nedd4-2 in mediating the cellular response to ER stress in neurons and could provide insight into other neurological diseases in which Nedd4-2 is dysregulated.

Questions remain regarding the mechanisms by which Nedd4-2 regulates the observed physiological changes in our study. To begin, although our study revealed the role of Nedd4-2 in the maintenance of neural activity and excitatory synapses upon induction of ER stress, it is unclear whether ER stress-induced translational suppression plays a role in these effects. To probe this question, one could utilize an integrated stress response (ISR) modulator known as ISRIB. ISRIB has been shown to rescue translation in the presence of phosphorylated eIF2α by facilitating the assembly of eIF2B (Rabouw *et al*. 2019). As our previous study demonstrated impaired translational suppression in *Nedd4-2* cKO cortical neuron cultures during ER stress (Eagleman *et al*. 2020), and our current study demonstrated impaired phosphorylation of eIF2α in the absence of Nedd4-2 during ER stress (Figure 4), it is possible that the observed physiological changes in Nedd4-2 cKO neurons are the result of improper translational regulation. If this were the case, we predict that treating *Nedd4-2* WT neurons with ISRIB prior to induction of ER stress would lead to phenotypic changes similar to those observed in the *Nedd4-2* cKO neurons in this study.

Another remaining question is how Nedd4-2 may mediate the phosphorylation of eIF2α. eIF2α is directly phosphorylated by several kinases: PERK (protein kinase R-like endoplasmic reticulum kinase), PRK (protein kinase double-stranded RNA-dependent), GCN2 (general control non-derepressible-2) and HRI (heme-regulated initiator) (Donnelly *et al*. 2013). Each of these kinases act to suppress translation in response to different cellular stressors. Because our study centered on ER stress, it is possible that impairments in eIF2α could be due to improper activation of PERK in the absence of Nedd4-2. Alternatively,

eIF2α phosphorylation is also mediated by multiple phosphatases including PPP3CA (Bollo *et al.* 2010). We have previously shown that PPP3CA is a direct ubiquitination substrate of Nedd4-2 (Zhu *et al.* 2019). Thus, Nedd4-2 could play a role in regulating PPP3CA during ER stress to affect eIF2α phosphorylation. It is important to test the above possibilities and determine whether Nedd4-2 plays a direct or indirect role in the regulation of eIF2α phosphorylation, as such data could provide evidence that Nedd4-2 is an integral component of the unfolded protein response.

Genetic knock-down of *Nedd4-2* has previously been shown to increase spontaneous neuronal activity and seizure susceptibility (Liu *et al.* 2021b; Zhu *et al.* 2017). Our study confirms this observation, as we persistently observed increased seizure burden in response to our low dose of kainic acid in the *Nedd4-2* cKO mice when compared to the *Nedd4-2* WT mice (Figure 5). The basally elevated seizure susceptibility in *Nedd4-2* cKO mice is known to be caused primarily by impaired ubiquitination of multiple ion channels (Zhu *et al.* 2017). However, it is also known that seizures can induce ER stress (Carnevalli *et al.* 2006) and our data have suggested a role for Nedd4-2 in ER stress–induced reduction of spontaneous firing rate. These seemingly contradictory data indicate a possibility that, while Nedd4-2 is crucial to lower basal neuronal activity, it also plays a role in ameliorating seizure-induced neuronal injury. By ameliorating such damage, Nedd4-2 could prevent the abnormal reduction of neuronal activity as we observed in this study. As a future direction, it would be particularly important to determine whether Nedd4-2 indeed plays a role in reducing neuronal degeneration and death following seizure insult.

Our data also indicate an uncoupling between eIF2α phosphorylation and reduction of seizure susceptibility in *Nedd4-2* cKO mice. This finding suggests that the absence of *Nedd4-2* might disrupt other downstream effectors of eIF2α phosphorylation and subsequently occlude the beneficial function of eIF2α phosphorylation in reducing seizure susceptibility. Our previous work has shown that, upon induction of ER stress in neurons, certain proteins are selectively synthesized, leading to homeostatic reduction of neural activity and seizure susceptibility (Liu *et al.* 2019). This selective protein synthesis might be facilitated by the elevated availability of ribosomes following global translation arrest through eIF2α phosphorylation. Following this notion, there is a possibility that Nedd4-2 may participate in selective protein synthesis following seizure-induced ER stress. This idea is supported by our previous work showing a role for Nedd4-2 in protein synthesis (Eagleman *et al.* 2020). If this is true, it could explain why promoting eIF2α phosphorylation alone using salubrinal is not sufficient to reduce seizure susceptibility in *Nedd4-2* cKO mice.

Lastly, it would be interesting to determine whether our findings can explain other pathophysiological conditions beyond seizures. Previous studies have shown that eIF2α phosphorylation is induced during ischemic stroke and Alzheimer's disease (Ma *et al.* 2013; Kumar *et al.* 2001). Interestingly, and perhaps not surprisingly based upon the dual nature of the unfolded protein response, phosphorylation of eIF2α is sometimes associated with increased neuronal death and other times is associated with increased neuronal survival. This duality is further exacerbated by studies showing benefits and drawbacks of salubrinal treatment in the face of neurological insults (Rubovitch *et al.* 2015; Huang *et al.* 2012; Gao

et al. 2013; Kim *et al*. 2014; Liu *et al*. 2019). Taken together, these results suggest that there is a Goldilocks' zone with regard to the ER stress response, which may be specific to the types and intensity of cellular insults. It would be interesting to determine what this ideal zone is in terms of neurological diseases that have been shown to be mediated by Nedd4-2.

Supplementary Material

Refer to Web version on PubMed Central for supplementary material.

ACKNOWLEDGEMENTS

We thank Tiffany Jong, Bailey Metcalf, and Jack Gerling for their technical assistance and Simon Lizarazo for statistical assistance. This work is supported by the National Institute of Health (R01NS105615 to N-P.T.) and by the American Heart Association Predoctoral Fellowship (20PRE35210705 to D.E.L.).

Abbreviations:

ATF4	Activating Transcription Factor 4
ATF6	Activating Transcription Factor 6
cKO	conditional knockout
CoxIV	Cytochrome c oxidase subunit 4 isoform 1
DIV	days-in-vitro
DMSO	Dimethyl sulfoxide
eIF2α	eukaryotic initiation factor-2α
ER	endoplasmic reticulum
HECT	homologous to the E6-AP C-terminus
IRE1α	Inositol-requiring enzyme 1α
MEA	multielectrode array
Nedd4-2	neural precursor cell expressed developmentally downregulated protein 4-like
PDI	Protein disulfide isomerase
PERK	protein kinase R-like endoplasmic reticulum kinase
PSD-95	post-synaptic density protein 95
Tg	Thapsigargin
UPR	unfolded protein response
WT	wild-type
XBP1	X-Box Binding Protein 1

REFERENCES

Binder JX, Pletscher-Frankild S, Tsafou K, Stolte C, O'Donoghue SI, Schneider R, Jensen LJ (2014) COMPARTMENTS: unification and visualization of protein subcellular localization evidence. Database 2014.

Bollo M, Paredes RM, Holstein D, Zheleznova N, Camacho P, Lechleiter JD (2010) Calcineurin Interacts with PERK and Dephosphorylates Calnexin to Relieve ER Stress in Mammals and Frogs. PLoS One 5, e11925. [PubMed: 20700529]

Carnevalli LS, Pereira CM, Jaqueta CB, Alves VS, Paiva VN, Vattem KM, Wek RC, Mello LEAM, Castilho BA (2006) Phosphorylation of the α subunit of translation initiation factor-2 by PKR mediates protein synthesis inhibition in the mouse brain during status epilepticus. Biochem. J 397, 187–194. [PubMed: 16492139]

Dibbens LM, Ekberg J, Taylor I, Hodgson BL, Conroy SJ, Lensink IL, Kumar S, et al. (2007) Nedd4-2 as a potential candidate susceptibility gene for epileptic photosensitivity. Genes, Brain Behav. 6, 750–755. [PubMed: 17331106]

Donnelly N, Gorman AM, Gupta S, Samali A (2013) The eIF2α kinases: Their structures and functions. Springer.

Donovan P, Poronnik P (2013) Nedd4 and Nedd4-2: Ubiquitin ligases at work in the neuron. Int. J. Biochem. Cell Biol 45, 706–710. [PubMed: 23262292]

Eagleman DE, Zhu J, Liu DC, Seimetz J, Kalsotra A, Tsai NP (2020) Unbiased proteomic screening identifies a novel role for the E3 ubiquitin ligase Nedd4-2 in translational suppression during ER stress. J. Neurochem September, 1–12.

Gao B, Zhang XY, Han R, Zhang TT, Chen C, Qin ZH, Sheng R (2013) The endoplasmic reticulum stress inhibitor salubrinal inhibits the activation of autophagy and neuroprotection induced by brain ischemic preconditioning. Acta Pharmacol. Sin 34, 657–666. [PubMed: 23603983]

Goel P, Manning JA, Kumar S (2015) Nedd4-2 (NEDD4L): The ubiquitin ligase for multiple membrane proteins. Gene 557, 1. [PubMed: 25433090]

Hetz C (2012) The unfolded protein response: Controlling cell fate decisions under ER stress and beyond. Nat. Rev. Mol. Cell Biol 13, 89–102. [PubMed: 22251901]

Hossain MM, Sivaram G, Richardson JR (2019) Regional susceptibility to ER stress and protection by salubrinal following a single exposure to deltamethrin. Toxicol. Sci 167, 145–156. [PubMed: 30203000]

Huang X, Chen Y, Zhang H, Ma Q, wu Zhang Y., Xu H (2012) Salubrinal attenuates β-amyloid-induced neuronal death and microglial activation by inhibition of the NF-κB pathway. Neurobiol. Aging 33, 1007.e9–1007.e17.

Hughes JR, Parsons JL (2020) The E3 Ubiquitin Ligase NEDD4L Targets OGG1 for Ubiquitylation and Modulates the Cellular DNA Damage Response. Front. Cell Dev. Biol 0, 1341.

Ingham RJ, Gish G, Pawson T (2004) The Nedd4 family of E3 ubiquitin ligases: functional diversity within a common modular architecture. Oncogene 2004 2311 23, 1972–1984.

Johnston MV, Ammanuel S, O'Driscoll C, Wozniak A, Naidu S, Kadam SD (2014) Twenty-four hour quantitative-EEG and in-vivo glutamate biosensor detects activity and circadian rhythm dependent biomarkers of pathogenesis in Mecp2 null mice. Front. Syst. Neurosci 8.

Kang SK, Ammanuel S, Thodupunuri S, Adler DA, Johnston MV, Kadam SD (2018) Sleep dysfunction following neonatal ischemic seizures are differential by neonatal age of insult as determined by qEEG in a mouse model. Neurobiol. Dis 116, 1. [PubMed: 29684437]

Kim JS, Heo RW, Kim H, ok Yi C., Shin HJ, Han JW, Roh GS (2014) Salubrinal, ER stress inhibitor, attenuates kainic acid-induced hippocampal cell death. J. Neural Transm 121, 1233–1243. [PubMed: 24728926]

Kim T, Chokkalla AK, Vemuganti R (2020) Deletion of ubiquitin ligase Nedd4l exacerbates ischemic brain damage: 10.1177/0271678X20943804 41, 1058–1066.

Kumar R, Azam S, Sullivan JM, Owen C, Cavener DR, Zhang P, Ron D, et al. (2001) Brain ischemia and reperfusion activates the eukaryotic initiation factor 2α kinase, PERK. J. Neurochem 77, 1418–1421. [PubMed: 11389192]

Lackovic J, Howitt J, Callaway JK, Silke J, Bartlett P, Tan SS (2012) Differential regulation of Nedd4 ubiquitin ligases and their adaptor protein Ndfip1 in a rat model of ischemic stroke. Exp. Neurol 235, 326–335. [PubMed: 22417925]

Lee D-E, Yoo JE, Kim J, Kim S, Kim S, Lee H, Cheong H (2020) NEDD4L downregulates autophagy and cell growth by modulating ULK1 and a glutamine transporter. Cell Death Dis. 2020 111 11, 1–17.

Lee KY, Jewett KA, Chung HJ, Tsai N-P (2018) Loss of fragile X protein FMRP impairs homeostatic synaptic downscaling through tumor suppressor p53 and ubiquitin E3 ligase Nedd4-2. Hum. Mol. Genet 27, 2805–2816. [PubMed: 29771335]

Liu D-C, Eagleman DE, Tsai N-P (2019) Novel roles of ER stress in repressing neural activity and seizures through Mdm2- and p53-dependent protein translation. PLOS Genet. 15, e1008364. [PubMed: 31557161]

Liu DC, Lee KY, Lizarazo S, Cook JK, Tsai NP (2021a) ER stress-induced modulation of neural activity and seizure susceptibility is impaired in a fragile X syndrome mouse model. Neurobiol. Dis 158, 105450. [PubMed: 34303799]

Liu X, Zhang H, Zhang B, Tu J, Li X, Zhao Y (2021b) Nedd4-2 haploinsufficiency in mice causes increased seizure susceptibility and impaired Kir4.1 ubiquitination. Biochim. Biophys. Acta - Mol. Basis Dis 1867, 166128. [PubMed: 33722745]

Lüttjohann A, Fabene PF, van Luijtelaar G. (2009) A revised Racine's scale for PTZ-induced seizures in rats. Physiol. Behav 98, 579–586. [PubMed: 19772866]

Ma T, Trinh MA, Wexler AJ, Bourbon C, Gatti E, Pierre P, Cavener DR, Klann E (2013) Suppression of eIF2α kinases alleviates Alzheimer's disease-related plasticity and memory deficits. Nat. Neurosci 16, 1299–1305. [PubMed: 23933749]

Manning JA, Kumar S (2018) Physiological Functions of Nedd4-2: Lessons from Knockout Mouse Models. Trends Biochem. Sci 43, 635–647. [PubMed: 30056838]

Rabouw HH, Langereis MA, Anand AA, Visser LJ, Groot R. J. de, Kuppeveld Walter P., van FJM (2019) Small molecule ISRIB suppresses the integrated stress response within a defined window of activation. Proc. Natl. Acad. Sci 116, 2097–2102. [PubMed: 30674674]

Rajesh K, Krishnamoorthy J, Gupta J, Kazimierczak U, Papadakis AI, Deng Z, Wang S, Kuninaka S, Koromilas AE (2016) The eIF2α serine 51 phosphorylation-ATF4 arm promotes HIPPO signaling and cell death under oxidative stress. Oncotarget 7, 51044. [PubMed: 27409837]

Rotin D (2008) Role of the UPS in Liddle syndrome. BioMed Central.

Rubovitch V, Barak S, Rachmany L, Goldstein RB, Zilberstein Y, Pick CG (2015) The Neuroprotective Effect of Salubrinal in a Mouse Model of Traumatic Brain Injury. NeuroMolecular Med. 17, 58–70. [PubMed: 25582550]

Shi PP, Cao XR, Sweezer EM, Kinney TS, Williams NR, Husted RF, Nair R, et al. (2008) Salt-sensitive hypertension and cardiac hypertrophy in mice deficient in the ubiquitin ligase Nedd4-2. 10.1152/ajprenal.90300.2008 295, 462–470.

Sokka A-L, Putkonen N, Mudo G, Pryazhnikov E, Reijonen S, Khiroug L, Belluardo N, Lindholm D, Korhonen L (2007) Endoplasmic Reticulum Stress Inhibition Protects against Excitotoxic Neuronal Injury in the Rat Brain. J. Neurosci 27, 901–908. [PubMed: 17251432]

Wang H, Sun RQ, Camera D, Zeng XY, Jo E, Chan SMH, Herbert TP, Molero JC, Ye JM (2016) Endoplasmic reticulum stress up-regulates Nedd4-2 to induce autophagy. FASEB J. 30, 2549–2556. [PubMed: 27022162]

Wang Y, Pan W, Bai X, Wang X, Wang Y, Yin Y (2021) microRNA-454-mediated Nedd4-2/TrkA/cAMP axis in heart failure: Mechanisms and cardioprotective implications. J. Cell. Mol. Med 25, 5082–5098. [PubMed: 33949117]

Yanpallewar S, Wang T, Koh DCI, Quarta E, Fulgenzi G, Tessarollo L (2016) Nedd4-2 haploinsufficiency causes hyperactivity and increased sensitivity to inflammatory stimuli. Sci. Reports 2016 61 6, 1–9.

Zhu J, Lee KY, Jewett KA, Man HY, Chung HJ, Tsai NP (2017) Epilepsy-associated gene Nedd4-2 mediates neuronal activity and seizure susceptibility through AMPA receptors. PLoS Genet. 13, e1006634. [PubMed: 28212375]

Zhu J, Lee KY, Jong TT, Tsai N (2019) C2-lacking isoform of Nedd4-2 regulates excitatory synaptic strength through GluA1 ubiquitination-independent mechanisms. J. Neurochem 151, 289–300. [PubMed: 31357244]

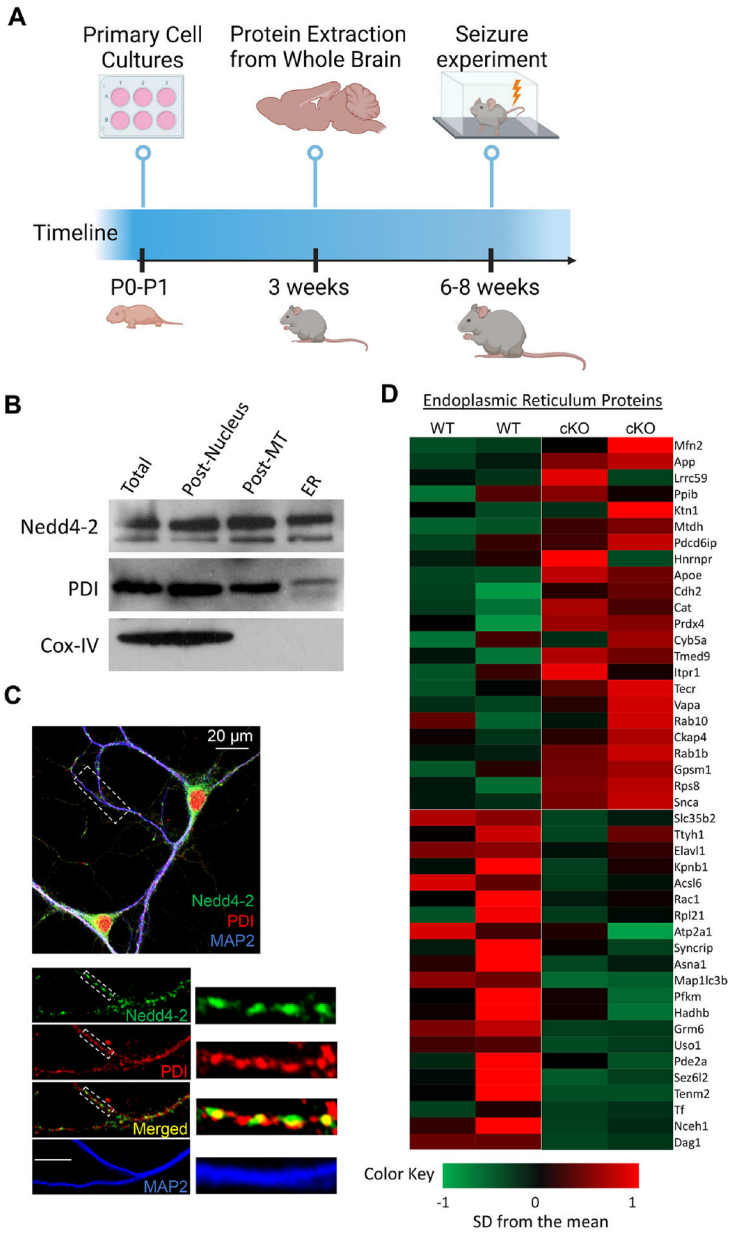

Figure 1. Nedd4-2 colocalizes with the endoplasmic reticulum and may regulate ER proteins.

(A) Timeline of the experimental procedures. (B) Representative western blots of Nedd4-2, protein disulfide isomerase (PDI; ER marker), and CoxIV (Cytochrome c oxidase subunit 4 isoform 1, mitochondrial marker) after isolation of rough ER enriched microsomes. This experiment was repeated three times. (C) Representative immunocytochemistry images showing colocalization of Nedd4-2 and PDI in WT neurons. (D) A heat map demonstrating altered expression of ER associated proteins derived from membrane fractions of the brains of *Nedd4-2* WT and *Nedd4-2* cKO mice following proteomic profiling.

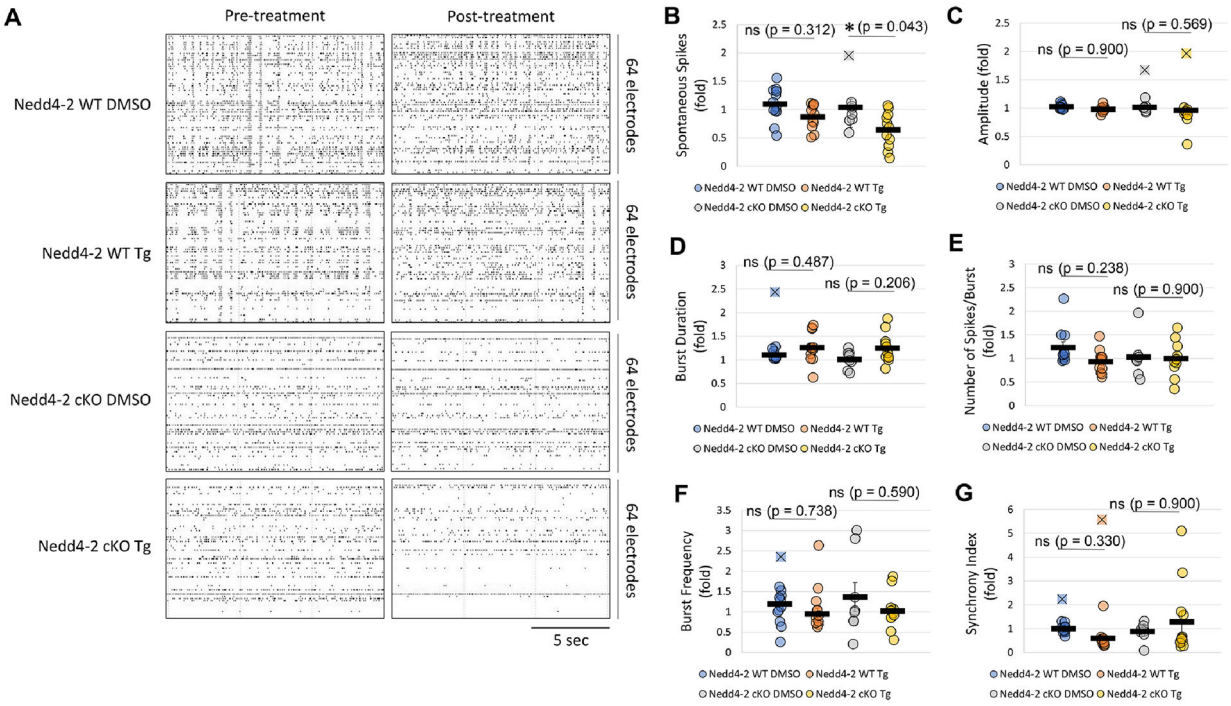

Figure 2. Induction of ER stress causes changes in spontaneous neural activity in *Nedd4-2* cKO cortical neuron cultures.

(A-E) Representative raster plots (A), quantifications of spontaneous spikes rate (B), spontaneous spike amplitude (C), burst duration (D), the number of spikes per burst (E), burst frequency (F), and synchrony index (G), after induction of ER stress using thapsigargin (Tg) (n=8–12). In all cases, data were obtained from at least 3 independent litters. The fold change is relative to the DMSO treated controls of each genotype. Data was analyzed using ANOVA ($F_{3,38} = 4.714$, $p = 0.007$ for panel B; $F_{3,40} = 0.653$, $p = 0.586$ for panel C; $F_{3,37} = 2.083$, $p = 0.119$ for panel D; $F_{3,36} = 1.374$, $p = 0.266$ for panel E; $F_{3,37} = 0.908$, $p = 0.446$ for panel F; $F_{3,37} = 1.270$, $p = 0.299$ for panel G) with *post-hoc* Tukey HSD test, and are represented as mean ± SEM. The significance after Tukey test is marked with *p<0.05 and ns: non-significant.

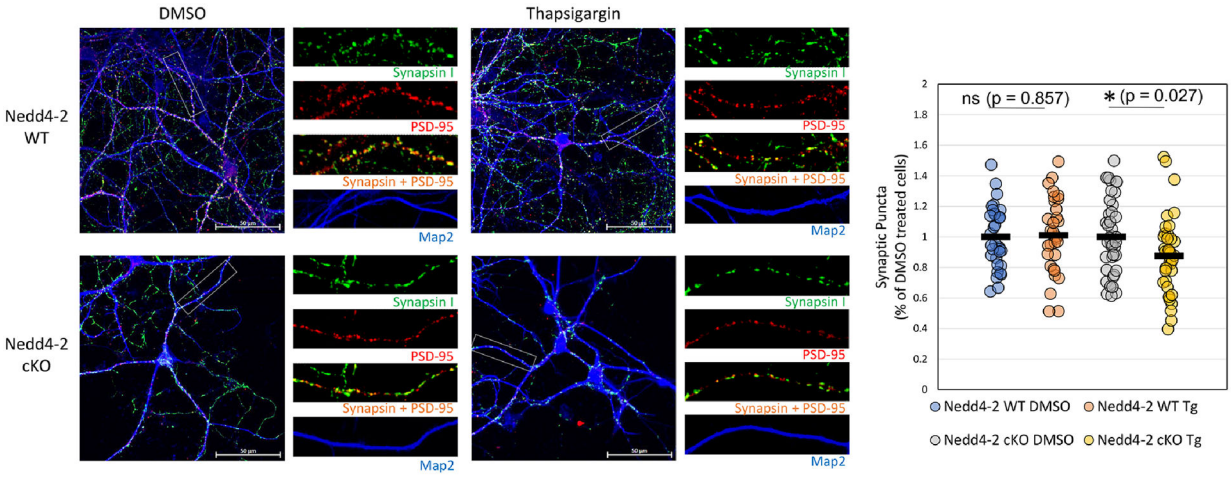

Figure 3. Nedd4-2 is required to maintain excitatory synapses during ER stress.

(Left) Representative images of immunocytochemistry showing synapsin I (green), PSD-95 (red), and Map2 (blue) in *Nedd4-2* WT and *Nedd4-2* cKO cortical neurons treated with DMSO or Tg for four hours. Magnified images of dendrites are shown to the right of the composite image. Scale bar: 50 μm. (Right) A quantification of the number of synaptic puncta in each condition (n=31–40 cells from three independent cultures). The fold change in synapse number is relative to the DMSO treated controls of each genotype. Data was analyzed using ANOVA ($F_{3,140} = 2.787$, $p = 0.043$) with *post-hoc* Tukey HSD test, and are represented as mean ± SEM. The significance after Tukey test is marked with *p<0.05 and ns: non-significant.

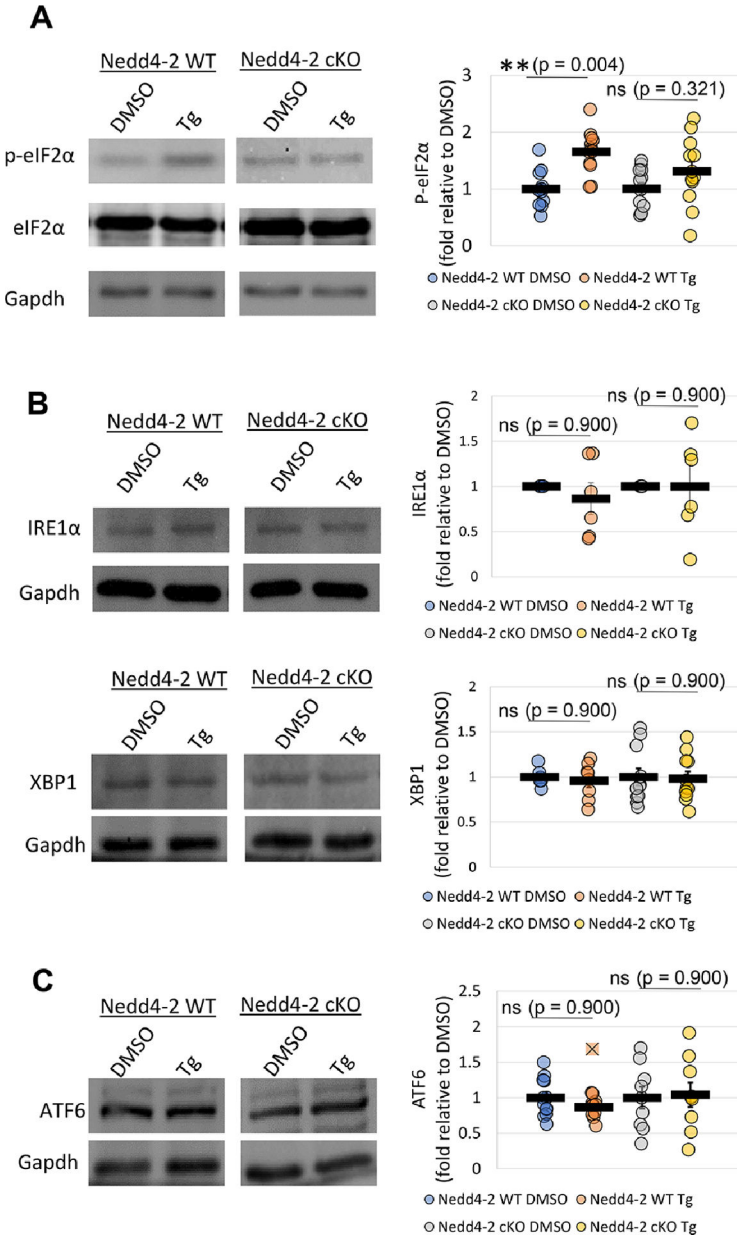

Figure 4. eIF2α phosphorylation upon induction of ER stress is impaired by genetic reduction of Nedd4-2.

(A) Representative western blots showing p-eIF2α and eIF2α in *Nedd4-2* WT and *Nedd4-2* cKO cortical neuron cultures after induction of ER stress (n=11 from 3 independent cultures for *Nedd4-2* WT DMSO; n=12 from 3 independent cultures for *Nedd4-2* WT Tg; n=12 from 3 independent cultures for *Nedd4-2* cKO DMSO and *Nedd4-2* cKO Tg). Quantification is on the right. (B) Representative western blots of IRE1α expression in *Nedd4-2* WT and *Nedd4-2* cKO cortical neuron cultures after induction of ER stress (n=6 from 6 independent cultures for all conditions) and XBP1 (n=6 from 3 independent cultures for *Nedd4-2* WT DMSO; n=8 from 3 independent cultures for *Nedd4-2* WT Tg; n=11 from 3 independent cultures for *Nedd4-2* cKO DMSO and *Nedd4-2* cKO Tg). Quantification is on the right. (C) Representative western blots of ATF6 expression in *Nedd4-2* WT and *Nedd4-2* cKO

cortical neuron cultures after induction of ER stress (n=11 from 3 independent cultures for *Nedd4-2* WT DMSO and *Nedd4-2* WT Tg; n=9 from 3 independent cultures for *Nedd4-2* cKO DMSO and *Nedd4-2* cKO Tg). Fold change is relative to DMSO treated controls of the same genotype. Data was analyzed using ANOVA ($F_{3,43} = 6.080$, $p = 0.002$ for panel A; $F_{3,20} = 0.226$, $p = 0.877$ for panel B; $F_{3,32} = 0.056$, $p = 0.982$ for panel C; $F_{3,38} = 0.143$, $p = 0.934$ for panel D) with *post-hoc* Tukey HSD test, and are represented as mean ± SEM. The significance after Tukey test is marked with **p<0.01 and ns: non-significant.

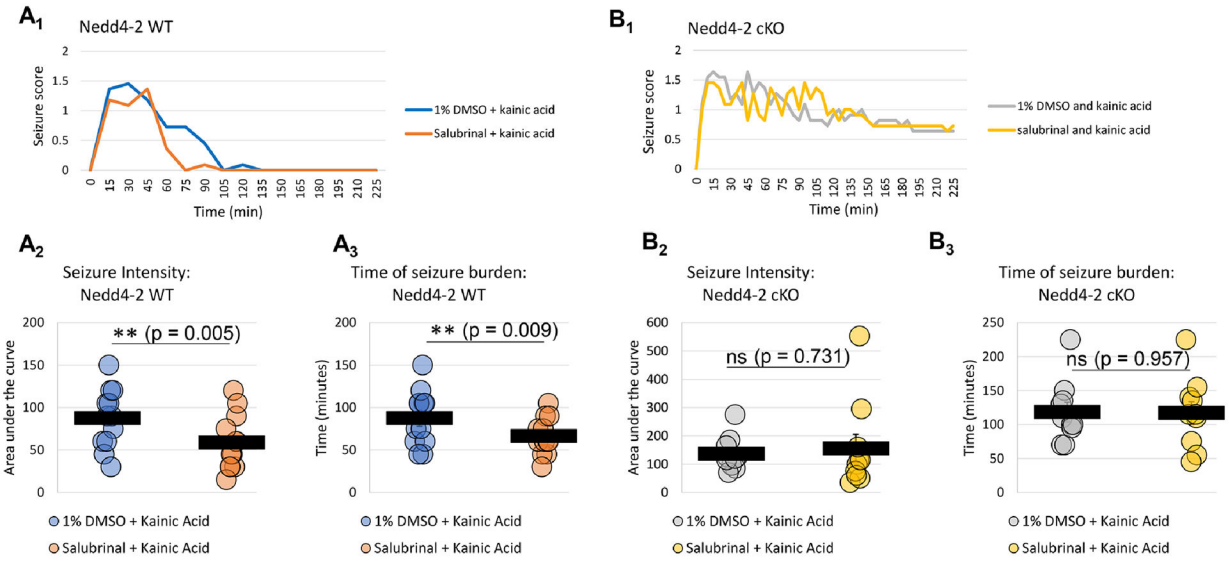

Figure 5. Salubrinal pre-treatment reduces seizure severity and duration in *Nedd4-2* WT but not *Nedd4-2* cKO mice.

(A_1) The pooled average of seizure scores across all *Nedd4-2* WT mice for the duration of observation. (A_2) Quantification of the area under the curve, serving as a measure of seizure intensity over time, for *Nedd4-2* WT mice (n=12 for each condition from 8 different litters). (A_3) Quantification of the time of seizure burden for *Nedd4-2* WT mice (n=12 for each condition from 8 different litters) (df = 22, t = ±2.074). (B_1) The pooled average of seizure scores across all *Nedd4-2* cKO mice for the duration of observation. (B_2) Quantification of the area under the curve, serving as a measure of seizure intensity over time, for *Nedd4-2* cKO mice (n=10 for each condition from 6 different litters). (B_3) Quantification of the time of seizure burden for *Nedd4-2* cKO mice (n=10 for each condition from 6 different litters) (df = 18, t = ±2.101). No animals were excluded in this experiment. Data was analyzed using Student's *t*-test, and are represented as mean ± SEM, with **p<0.01 and ns: non-significant.

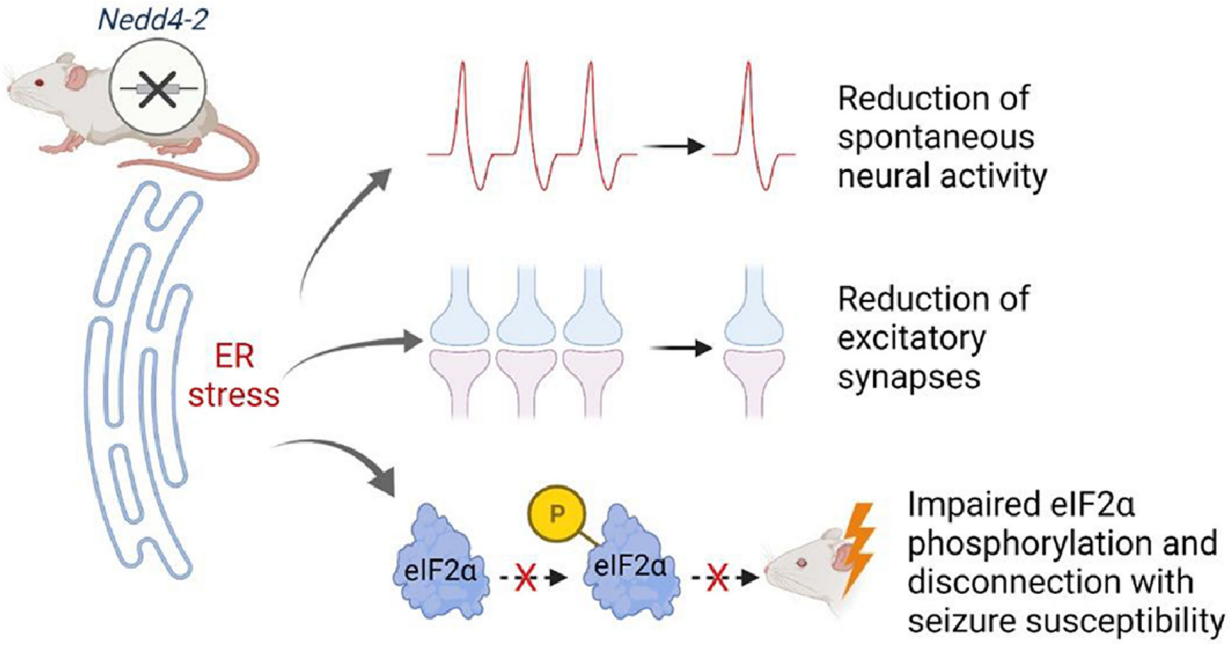

Figure 6. A working model for the neuroprotective activities of Nedd4-2 during ER stress.

In *Nedd4-2* cKO cortical neuron cultures, induction of ER stress leads to a reduction in spontaneous neural activity, a reduction of excitatory synapses, and impaired eIF2α phosphorylation. This impairment in eIF2α phosphorylation coupled with *Nedd4-2* deletion in mice causes a defect that impairs pharmacological reduction in seizure susceptibility mediated by salubrinal.